Journal of Electroceramics, 13, 139–147, 2004

Pyroelectric Arrays: Ceramics and Thin Films

ROGER W. WHATMORE*

School of Industrial and Manufacturing Sciences, Cranfield University, Cranfield, Bedfordshire, MK43 0AL, UK

Submitted July 14, 2004; Revised August 6, 2004; Accepted August 10, 2004

Abstract. Pyroelectric infra-red detectors have been of-interest for many years because of their wide wavelength response, good sensitivity and lack of need for cooling. They have achieved a wide market acceptance for such applications as people sensing, IR spectrometry (especially for environmental protection) and flame/fire protection. Arrays of such detectors, comprising a pyroelectric material interfaced to an application specific integrated circuit for signal amplification and read out, provide an attractive solution to the problem of collecting spatial information on the IR distribution in a scene and a range of new applications are appearing for such devices, from thermal imaging to people sensing and counting. The selection of the best material to use for such a device is very important. Because all polar dielectrics are pyroelectric, there is a very wide range of such materials to choose. The performance of a pyroelectric IR sensor array can be derived from the physics of their operation and figures-of-merit (FoM) defined that will describe the performance of a material in a device, in terms of its basic pyroelectric, dielectric and thermal properties. These FoM and their appropriateness for the array application are reviewed. Large arrays of small detectors are best served by the use of pyroelectric materials with permittivities between 200 and 1000, depending upon the element size and the element thermal conductance, and a maximised FoM $F_D = p\{c'(\varepsilon\varepsilon_o \tan\delta)^{1/2}\}$. Such properties are found in ferroelectric perovskite ceramics and a wide range have been explored for their use in pyroelectric arrays. These include materials based on compositions in the $PbZr_xTi_{1-x}O_3$ (PZT) system, for example close to $PbZrO_3$, with Curie temperatures well above ambient. Examples of the ways in which these materials can be modified by doping to optimise their FoM and other important properties such as electrical resistivity are given and the physics operating behind this discussed. The performances and costs of uncooled pyroelectric arrays are ultimately driven by the materials used. For this reason, continuous improvements in materials technology are important. In the area of bulk ceramics, it is possible to obtain significant improvements in both production costs and performance though the use of tape-cast, functionally-gradient materials. Finally, the use of directly-deposited ferroelectric thin films on silicon ASIC's is offering considerable potential for low cost high performance pyroelectric arrays. The challenges involved in developing such materials will be discussed, especially from the aspect of low temperature deposition and other fabrication issues, such as patterning. Sol gel deposition provides an excellent technique for thin film growth and Mn-doped PZT films can be grown at 560°C with a FoM F_D exceeding those of many bulk materials.

1. Introduction

The pyroelectric effect, whereby a polar dielectric will generate charge when it is heated, has been known for hundreds (if not thousands) of years, as has been reviewed by Lang [1]. The first suggestion for the application of the effect to infra-red detection was by Ta in 1938 [2]. In such pyroelectric infra-red (PIR) detectors, the infra-red energy is absorbed in a thin chip of the pyroelectric material, the resulting temperature change giving-rise to a pyroelectric current, that can be detected in an external circuit. Since then, detectors have been demonstrated working from the visible

*E-mail: rw.whatmore@cranfield.ac.uk

[3] through the infrared [4] to sub-millimetre [5] and millimetre [6] wavelengths. They have also been used at radiation modulation frequencies from a few hertz [4] to many gigahertz [7]. The volume applications of pyroelectric infra-red detectors lie in the 8–12 micron atmospheric window, where their use as people detectors in applications such as burglar alarms and remote light switches will be familiar to many people. Here, their advantages of room-temperature operation, broad wavelength response, high stability and high sensitivity in comparison with other thermal detectors such as thermopiles or resistive bolometers, coupled with very low cost have combined to give them complete dominance in the market-place. These devices usually consist of single or dual elements in a simple transistor-type package, incorporating a window that is transparent over the wavelength range of-interest. Other applications for such devices include flame and fire detectors and low-cost spectroscopic gas analysers where the window on the front of the detector is selected and/or coated to make the device sensitive at the wavelength of-interest. The basic design of a pyroelectric detector is shown in Fig. 1. The thin pyroelectric element is connected to a high input impedance amplifier, typically a field-effect transistor. The pyroelectric current, i_p generates a voltage V_p across the electrical admittance Y_E presented to it. The circuit show is a unity-gain voltage amplifier that effectively couples the high impedance source of current (the pyroelectric element) to a low input impedance following circuit.

Over the last few years there has been a remarkable growth of interest in arrays of pyroelectric elements for a variety of applications such as thermal imaging [8] in applications such as fire-fighting [9]. These have been made using a thin ferroelectric ceramic wafer is bonded to a 2D array of amplifiers and multiplexer switches integrated on an application specific silicon read-out integrated circuit (ROIC). Companies such as BAE SYSTEMS Infra-red Ltd. in the UK have developed arrays with 128 × 256 and 384 × 288 elements [8], while Raytheon in the USA have developed an array with 320 × 240 elements [10]. In the last few years there has been a growth of interest in the use of low cost arrays of a few-hundred elements in applications such as people sensing/counting and imaging radiometry [11]. The potential for integrating ferroelectric thin films directly onto silicon substrates has been recognised as a means for both reducing array fabrication costs and increasing performance through reduced thermal mass and improved thermal isolation. This has encouraged the development of fully integrated 2D arrays and encouraged the low temperature (<550°C) growth of ferroelectric thin films such as lead zirconate titanate (PZT) directly onto active silicon devices [12].

The purpose of this paper is to review the issues associated with the selection of pyroelectric materials in such applications, with particular reference to the use of ferroelectric ceramics and thin films.

2. Pyroelectric Device Operation and Materials Properties

The operation and device physics of PIR detectors has been extensively reviewed elsewhere [4, 8, 13, 14] and hence only the salient features of device operation as pertaining to pyroelectric materials selection will be discussed. In the case of a device structured as

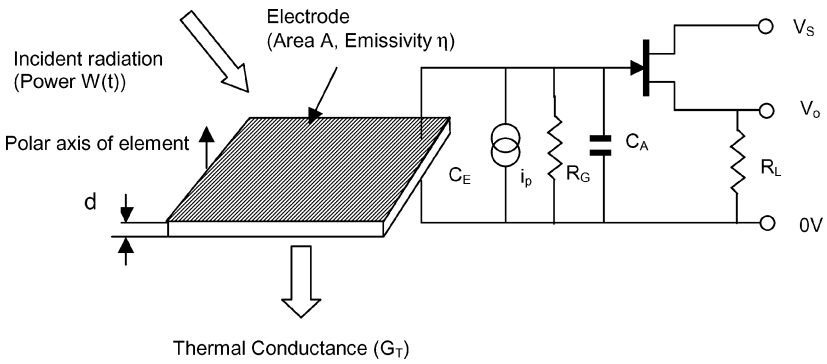

Fig. 1. Schematic diagram of a pyroelectric detector element.

in Fig. 1, we can determine i_p in terms of the average IR power (described as a sinusoidally modulated signal $W(t) = W_o \exp(i\omega t)$) incident upon the pyroelectric element. The pyroelectric current is given by $i_p = Apd\theta/dt$, where A is the area of the pyroelectric element, p is the pyroelectric coefficient and $d\theta/dt$ is the rate of change of the element temperature (θ) with time. This expression immediately tells us that the PIR detector only responds to *changes* in element temperature with time, and that i_p is maximised by firstly maximising the active area of the element, within whatever other device constraints there may be (larger area detectors tend to be intrinsically more sensitive) and that material with a larger p will produce more charge, and hence more current. In order to determine the expression for the "current responsivity" ($R_i = i_p/W_o$), we need to describe the balance between power input to the element ($\eta W(t)$), power retained by the element ($Hd\theta/dt$ where H is the element thermal capacity), and power lost to the environment ($G\theta$). If we do this, we can show that

$$\frac{i_p}{W_o} = R_i = \frac{\eta p A \varpi}{G_T\left(1 + \varpi^2 \tau_T^2\right)^{1/2}}.$$

At high modulation frequencies ($\omega > 1/\tau_T$, where $\tau_T = H/G$, the thermal time constant of the element), $R_i = \frac{\eta pA}{H} = \frac{\eta p}{c'd}$ (c' = volume specific heat of the element material). Hence, under these conditions, the current responsivity is proportional to a factor which depends only on the pyroelectric and thermal properties of the material used to make-up the active element. This "figure of merit" (FoM) is F_i, where $F_i = \frac{p}{c'}$. Most devices are, however, voltage-mode—as shown in Fig. 1. To derive the voltage responsivity, $R_V = V_p/W_o$, we need to consider the electrical admittance presented to i_p. If this is done, we can show that

$$R_V = \frac{i_p}{\mathrm{Y} W_o} = \frac{R_G \eta p A \varpi}{G_T\left(1 + \varpi^2 \tau_T^2\right)^{1/2}\left(1 + \varpi^2 \tau_E^2\right)^{1/2}}.$$

Here, τ_E is the electrical time constant ($\tau_E = R_G(C_E + C_A)$). The general form of this response (on a log/log graph) is a rising response at low frequencies, a fairly flat response (varying by only 3dB) between the two frequencies represented by $1/\tau_E$ and $1/\tau_T$, and then a $1/\omega$ roll-off above this. In the high frequency region, the response can be shown to be $R_V = \frac{\eta p}{c' \varepsilon \varepsilon_o A \varpi}$ (provided $C_E \gg C_A$) and we can thus describe the performance under these conditions as being proportional to a material FoM F_V, where $F_V = \frac{p}{c' \varepsilon \varepsilon_o}$. Finally, for most purposes we are most interested in signal-to-noise ratio. The performances of detectors are frequently described in terms of their specific detectivity, D^*, where $D^* = \frac{A^{1/2} R_V}{\Delta V_N}$. ΔV_N is the total RMS electrical noise and is the sum of all the noise contributions in the circuit shown in Fig. 1. These include the noise due to random fluctuations in the radiation incident on the detector, the current and voltage noise in the FET amplifier, and the Johnson noise in the AC impedance in parallel with the detector element. At frequencies above about 20 Hz, the latter dominates the total noise, so that the D^* is given by

$$D^* = \frac{R_V A^{1/2}}{\Delta V_J} = \frac{\eta d}{(4kT)^{1/2}} \frac{p}{c'(\varepsilon \varepsilon_o \tan \delta)^{1/2}} \frac{1}{\varpi^{1/2}}.$$

This gives the third material FoM generally used in discussing pyroelectric materials, F_D, where $F_D = \frac{p}{c' \sqrt{\varepsilon \varepsilon_o \tan \delta}}$.

It should be stressed in any discussion of FoM that it is essential that the dielectric properties are measured at a frequency similar to the range in which the pyroelectric device is to be used. This is because the dielectric properties, especially the dielectric loss, are frequency dependent. Most pyroelectric devices are used in the range of a few Hz (or below) up to 100 Hz. Hence, the dielectric properties should ideally be measured over this range, or in the centre of it. Unfortunately, many papers in the literature that discuss pyroelectric materials report dielectric properties measured at 1KHz, which will usually radically underestimate the loss at frequencies of a few Hz (sometimes by a factor of 4). The literature should be read with this consideration in mind.

It should be clear from the above discussion that, although the three FOM, F_i, F_V and F_D are useful in a rather "broad-brush" sense, in that they allow us to discuss and compare the properties of different pyroelectric materials, they are also rather limited in their usefulness. For example, F_i is only applicable for current-mode devices at high frequencies. F_V only applies at high frequencies when $C_E \gg C_A$. If $C_A \gg C_E$, for example, F_i would be a more-useful FOM to use. Ideally, we would wish to match C_E to be approximately equal to C_A. F_D is only useful if the AC Johnson noise in the element dominates the total noise. If this were not the case (as is true at low frequencies, or if the front-end electronics is "noisy"), then F_V would be a better FOM to use to compare different pyroelectric materials.

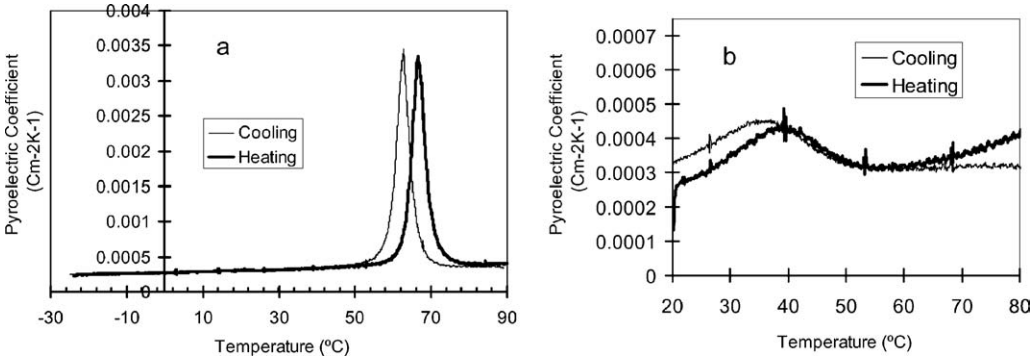

Fig. 2. Pyroelectric coefficient vs temperature for (a). $Pb(Zr_{0.85}[Mg_{1/3}Nb_{2/3}]_{0.075}Ti_{0.075})_{0.99}Mn_{0.01}O_3$ and (b). $Pb(Zr_{0.85}[Mg_{1/3}Nb_{2/3}]_{0.175}Ti_{0.075})_{0.99}Mn_{0.01}O_3$.

A particular case to consider is that of an appropriate material to use for a solid-state array of detectors, say for use in thermal imaging. Here, one is restricted in the size of the elements by the overall size of the ROIC that can be used. The maximum size of active silicon that it would be desirable to use for a ROIC would be ca. 1 cm $\times$ 1 cm. If, say, we wished to fit 100 $\times$ 100 elements into this area, then each element will be on a pitch of ca 100 μm and ca 80 μm square. If we want $C_E \approx C_A$, and $C_A \approx$ 1pF, then this value, together with the area and the thickness of the element allows us to determine the ideal permittivity of the pyroelectric material, regardless of the values of the FOM. Interestingly, we can determine the ideal thickness of the element by considering the thermal conductance of the element to the environment. If we consider an element design as shown in Fig. 2, with a conductive metal bump linking the active area to the ROIC, then for bumps of the order of 20 μm in diameter and 20 μm high, with a polymer thermal barrier layer, the conductance is ca 10 μW/K [8]. We want to design the system so that the thermal time constant is roughly 1/frame rate. Hence, for a 50 Hz frame rate we get $\tau_T = 20$ ms. It is possible to show that for this thermal time constant, with $c' \approx 2.7 \times 10^6$ Jm^{-3} K^{-1}, then $d = 25$ μm for an 80 μm square element. This implies that we need a permittivity (ε) of about 400. If the elements are only half this size (40 μm square) then we need a correspondingly-higher permittivity (ca. 1000). These permittivities must be maintained while still maximizing the appropriate FOM. Such high permittivities, coupled with acceptable FOM are generally found in the ferroelectric perovskites, which are most-conveniently available as ceramics or, more recently, as thin films deposited directly onto silicon.

While the pyroelectric, dielectric and thermal properties of pyroelectric materials are clearly fundamental in determining the basic performance of a device, there are many other properties to be considered when making a selection of an appropriate material. These are:

(i) Electrical resistivity: The circuit in Fig. 1 shows a resistor R_G connected across the active element. This serves two functions. Firstly, it fixes the electrical time constant τ_E of the device. Second, it allows the gate leakage current of the FET to bias its operating point. If there was no bias resistor here, the FET amplifier would not be stable and would take a long time to settle. Thirdly, it determines the voltage responsivity (see above). For $\varepsilon = 300$ and $\tau_T = 10$ s, then $\rho = \tau_T/\varepsilon\varepsilon_o \approx 3 \times 10^9$ Ωm. This would give a good compromise between settling time and R_V.

(ii) Piezoelectric properties: At first sight it seems surprising that the piezoelectric properties are important in pyroelectric devices. However, all pyroelectric detectors used in a high vibration or acoustically noisy environment will produce a piezoelectric microphonic noise signal, mostly through flexure, which can be very significant if steps are not taken to suppress it. Shorrocks et al. [15] have discussed methods by which the microphony of pyroelectric arrays may be reduced to a low level through good package design. The selection of a ceramic material that has a low d_{31} coefficient could be a valuable consideration.

(iii) Manufacturability: The ability to make the selected material in a large area at low cost is a

very important consideration. Ferroelectric ceramics have an important advantage here over some of the single crystal materials that are available, as a consequence of their relative ease of manufacture using a range of techniques and their stability during other subsequent manufacturing processes.

Ferroelectric ceramic materials allow us to achieve many of the desired properties for use in pyroelectric infra-red etector arrays and the rest of this paper will discuss some of the more-recent developments in this topic.

3. Pyroelectric Ceramics

There are two main classes of pyroelectric ceramics that are used commercially in infra-red detector arrays: ceramics with a Curie temperature T_C well above ambient (typically $>200^\circ$C), so that the pyroelectric coefficient is reversible and stable and ceramics with a T_C around room temperature, for which the pyroelectric coefficient must be stabilised by the application of a DC electric field. The latter group are frequently referred to as dielectric bolometers. The most widely used ceramics in the former group are those based on modified lead zirconate (PZ) [16, 17, 22] and those base on modified lead titanate [18]. (The morphotropic phase boundary compositions of the PZT system are generally avoided for pyroelectric applications because these have high permittivities, which are detrimental to the figures-of-merit). The FoM for a selection of compositions in these two classes of material are quite similar and are shown in Table 1. The pyroelectric properties of some of the materials that have been explored for dielectric bolometer applications are also given in Table 1. Because the latter have to be used under an applied bias field it is necessary to quote the temperature and field under which the relevant property measurements have been made. This is done here. It can be seen that significant improvements in FoM (factor of 2 to 3 in F_D) have been obtained by using a material such as lead scandium tantalate (PST) relative to what can be achieved using, for example, modified PZ. However, the conventional pyroelectric ceramics are still favoured for most practical applications because of the stability of their properties over the normal operating temperature range and because they do not need an applied DC bias field to operate them. The dielectric bolometer materials are preferred for thermal imaging arrays with large numbers of very small elements because of the need for high permittivities coupled with high F_D. The recent developments in dielectric bolometer materials have been adequately reviewed elsewhere [8, 19, 20] and will not be discussed further here.

There have been various experiments to try to improve the figures of merit of modified PZ compositions. One prospect is through exploitation of the step in the spontaneous polarisation at the $F_{R(LT)}$ to $F_{R(HT)}$ phase transition [21]. This leads to a significant increase in the pyroelectric coefficient over a relatively narrow temperature range, with very little change in the dielectric permittivity or loss in the same range. This produces a significant improvement in the pyroelectric FoM. Shaw et al. have studied this phase transition in the $PbZrO_3$-$PbTiO_3$-$PbMg_{1/3}Nb_{2/3}O_3$ system [22]. Figure 2 shows this peak for two compositions with the general formula $Pb(Zr_{0.925-y}[Mg_{1/3}Nb_{2/3}]_yTi_{0.075})_{0.99}Mn_{0.01}O_3$ with $y = 0.075$ and $y = 0.175$.

The large peak in the pyroelectric coefficient relative to the room temperature value is clearly visible.

Table 1.

Material	Meas. (°C)	$p10^{-4}$ (Cm^{-2} K^{-1})	DielectricProperties ε	tanδ	Freq. (Hz)	c' 10^6 (Jm^{-3} K^{-1})	T_C (°C)	F_V (m^2 C^{-1})	F_D 10^{-5} ($Pa^{-1/2}$)	Ref.
Mod. PZ (a)	25	4.0	290	0.003	1000	2.6	230	0.06	5.8	16
			300	0.014	33			0.06	2.6	
Mod. PZ (b)	25	3.56	218	0.007	33	2.6	226	0.07	5.1	22
Mod. PT	25	3.5	220	0.01	1000	2.6	>250	0.07	3.2	14
			220	0.03	33			0.07	1.8	
PST (d)	30	15	500	0.005	33	2.6	30		13	19
BST67/33 (e)	25	70	8800	0.004	1000	2.6	25		12.4	20

Compositions: (a) = $Pb(Zr_{0.58}Fe_{0.2}Nb_{0.2}Ti_{0.02})_{0.995}U_{0.005}O_3$; (b) = $Pb(Zr_{0.8}[Mg_{1/3}Nb_{2/3}]_{0.125}Ti_{0.075})_{0.99}Mn_{0.01}O_3$, PST = $PbSc_{0.5}Ta_{0.5}O_3$; (d) Measured at 5 V/μm; (e) Measured at 0.6 V/μm.

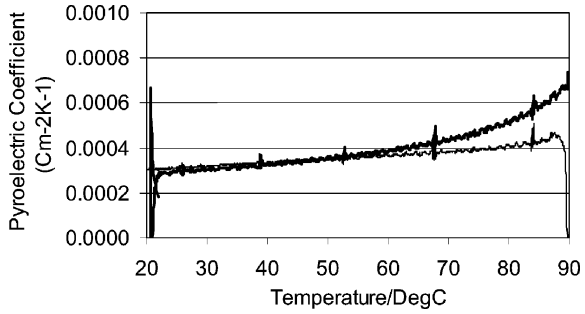

Fig. 3. Pyroelectric coefficient vs temperature for $Pb(Zr_{0.85}[Mg_{1/3}Nb_{2/3}]_{0.075}Ti_{0.125})_{0.99}Mn_{0.01}O_3$.

For $y = 0.075$, the value at the peak is a factor of 10 greater than at room temperature. However, the fact that the transition is first-order in nature means that there is significant thermal hysteresis, which means that this large peak is unusable for thermal detection. Furthermore, the transition is at too high a temperature (66°C on heating). The addition of more $PbMg_{1/3}Nb_{2/3}O_3$ so that $y = 0.175$ dramatically reduces both the $F_{R(LT)}$ to $F_{R(HT)}$ phase transition temperature and the degree of thermal hysteresis. It also makes the transition much more diffuse so that the increase occurs over a wider temperature range, but the magnitude of the peak is reduced so that it is now 50% greater than the room temperature value,. However this is still a useful increase. At higher amounts of Ti, the transition is increased to move well outside the temperature range of interest, as shown for $Pb(Zr_{0.80}[Mg_{1/3}Nb_{2/3}]_{0.075}Ti_{0.125})_{0.99}Mn_{0.01}O_3$ in Fig. 3. The temperature dependence of the dielectric properties going through the transition for composition $Pb(Zr_{0.85}[Mg_{1/3}Nb_{2/3}]_{0.075}Ti_{0.075})_{0.99}Mn_{0.01}O_3$ are shown in Fig. 4. The properties of the best composition in this series, which does not show the $F_{R(LT)}$ to $F_{R(HT)}$ phase transition is given in Table 1 and is $Pb(Zr_{0.80}[Mg_{1/3}Nb_{2/3}]_{0.125}Ti_{0.075})_{0.99}Mn_{0.01}O_3$. The p/ε ratio is reasonably constant from 0 to 70°C, leading to a constant voltage responsitivity, a useful characteristic, and the pyroelectric FoM are very good.

It was noted above that the ability to control the electrical resistivity in these ceramics is an important capability. For the perovskite oxide group (with the general formula ABO_3), to which PZT belongs, doping the 'B' site with uranium has previously been used [23] to alter the resistivity and ageing characteristics of a morphotropic phase boundary composition of PZT. Whatmore and co-workers [24, 25] reported the effects of uranium doping on the pyroelectric and resistive properties in the PZ-PT-PFN ceramic system. Their work on two quite different basecompostions $Pb(Zr_{0.76}Fe_{0.10}Nb_{0.10}Ti_{0.04})_{1-x}U_xO_3$ and $Pb(Zr_{0.68}Fe_{0.14}Nb_{0.14}Ti_{0.04})_{1-x}U_xO_3$ confirmed the wide applicability of this dopant to control both resistivity and dielectric constant and loss. This work showed that the uranium dopant resides on the B site, acting as a deep-level electron donor, compensating for the acceptors due to Pb vacancies. In this case, the conductivity is mediated by electron hopping, and it has been shown [26] that this is controlled by the activation energy for thermally-activated hopping conduction between carrier trapping sites within the crystal lattice of the ceramic grains. In this case the probability of a charge carrier hopping between two sites separated by a distance R due to the absorption of a phonon would be proportional to $\nu \exp(-\alpha R)$, where α is a constant at constant temperature and ν is a factor dependent upon phonon frequencies.

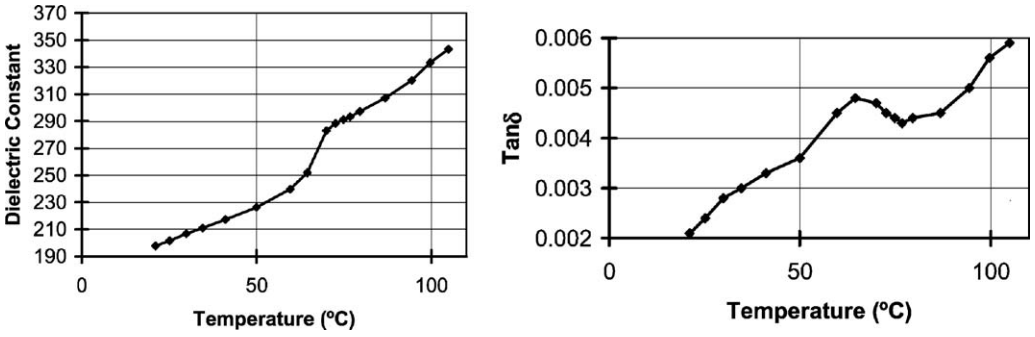

Fig. 4. Dielectric constant and loss as functions of temperature for $Pb(Zr_{0.85}[Mg_{1/3}Nb_{2/3}]_{0.075}Ti_{0.075})_{0.99}Mn_{0.01}O_3$.

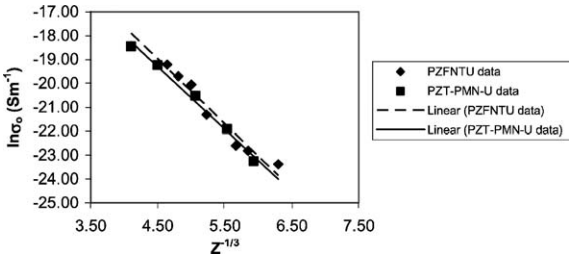

Fig. 5. Variation in log conductivity with doping of uranium (z) in two sets of pyroelectric ceramics from the $PbZrO_3$-$PbTiO_3$-$PbMg_{1/3}Nb_{2/3}O_3$ (PZFNTU) ($Pb\{(Mg_{1/3}Nb_{2/3})_{0.025}(Zr_{0.825}Ti_{0.175})_{0.975}\}_{1-z}U_zO_3$) and $PbZrO_3$-$PbTiO_3$-$PbFe_{1/2}Nb_{1/2}O_3$ (PZT-PMN-U) ($Pb(Zr_{0.58}Fe_{0.20}Nb_{0.20}Ti_{0.02})_{1-x}U_xO_3$) systems. Also shown are the linear fits to the function in Eq. (2) for the two compositions.

If the trapping sites are located at the dopant ions, as would be expected if the dopants were not ionised, then R is determined by the uranium oxide doping level, such that:

$$R = z^{-1/3}a \tag{1}$$

where a is the lattice parameter. Then for electron hopping conduction the DC conductivity (σ_o) should be given by:

$$\sigma_o = A\exp(\alpha a z^{-1/3} - E_a/kT) \tag{2}$$

where A is a constant.

Plotting $\ln\sigma_o$ against $z^{-1/3}$ (Fig. 5) for the resistivity data from a set of ceramics with the composition $Pb\{(Mg_{1/3}Nb_{2/3})_{0.025}(Zr_{0.825}Ti_{0.175})_{0.975}\}_{1-z}U_zO_3$ [27] gives a similar graph to that reported previously for ceramics in the uranium doped PZ-PT-PFN system with composition $Pb(Zr_{0.58}Fe_{0.20}Nb_{0.20}Ti_{0.02})_{1-x}U_xO_3$ [26]. Figure 5 also plots the data from this earlier study on the uranium-doped PZ-PT-PFN system, for the purposes of comparison. The similarity between the two sets of data is remarkable and shows that similar basic mechanisms are at work in each. Recently [28] it has been shown that Cr can act in a similar way to control electrical conductivity and that the carrier hopping can be described by the same theory.

An alternative technique to potentially improve the performance of pyroelectric materials is to structure them in an advantageous way. For example, one way to increase the width over which the effective width of the $F_{R(LT)}$ to $F_{R(HT)}$ phase transition occurs is to mix two or more ceramic compositions that have slightly different compositions, arranged to give different transition temperatures and to sinter them in such a way as to maintain the compositions. Wu et al. [29] have achieved this using spark source sintering of two ceramic compositions in the $PbZrO_3$-$PbTiO_3$-$PbZn_{1/3}Nb_{2/3}O_3$ system and shown pyroelectric coefficients as high as 10^{-3} Cm^{-2} K^{-1}, flat over the range 24 to 43°C. A similar effect can be achieved by laminating and co-sintering layers of ceramic with different compositions [30], forming a functionally-gradient material. Navarro et al. [31] have studied a different kind of functionally-gradient material in which a porous layer is included in the centre of a laminated stack. This reduces the average volume specific heat of the material while also reducing the thermal conductivity. They shown that in a three layer stack where two dense layers sandwich a single porous layer, each layer being 100 μm thick, with a porosity of ca 5% in the central layer, it is possible to increase F_V from ca 5×10^{-2} m^2 C^{-1} in the dense material to $> 8 \times 10^2$ m^2 C^{-1}.

4. Pyroelectric Thin Films

The use of bulk ferroelectrics in pyroelectric devices inevitably leads to a situation where the material must be cut, lapped and polished to make a thin, thermally-sensitive layer. If an array of detectors is required for thermal imaging, this must be metallised on both faces, processed photolithographically and bonded to a silicon read-out circuit to yield a complete hybrid array. Clearly, it would be desirable if the ferroelectric material could be deposited as a thin film, to remove the requirement for lapping and polishing, if possible directly onto a complete wafer of silicon chips, where it could be processed to yield an array of thin, thermally isolated structures [9]. As noted above, this means that the layer must be grown at ca 550°C or below. The oxide materials (modified lead zirconate titanates or the dielectric bolometer materials) which were discussed in the previous two sections possess the right properties (high dielectric constants and high values of F_D), but they are normally manufactured as ceramics and the sintering temperatures for these are around 1200°C. Fortunately, many techniques have been researched for ferroelectric thin film deposition, mainly for applications to non-volatile memories. These include chemical solution deposition (CSD)—particularly sol-gel or

metal-organic deposition (MOD), RF magnetron sputtering, pulsed laser ablation (PLD) and metal-organic chemical vapour deposition (MOCVD). Zhang et al. [32] have studied the low temperature fabrication of PZT and PMZT thin films annealed at 530 and 560°C. The dielectric constant and tangent loss of the PMZT films annealed at 530°C were 260 and 0.006 at 100 Hz and 257 and 0.0067 at 1 kHz, respectively. Under similar processing conditions, PZT thin films exhibit a dielectric constant of ∼360 and tangent loss of 0.01. In comparison with PZT thin film with similar thickness, Mn doped PZT thin film has a lower dielectric constant and a lower or equivalent tangent loss, which is of great significance in enhancing the performance of an infrared detector. Most PZT thin films have a pyroelectric coefficient of 1–2 $\times$ 10^{-4} CK^{-1} m^{-2} [9]. This improvement is due to the significant reductions in dielectric constant and loss and the improvements in the pyroelectric coefficient. It seems likely that both of these improvements can be ascribed to the fact that the Mn acts as a 'hardening' dopant in the PZT lattice, creating oxygen vacancies and pinning the residual domains. It is likely that the internal bias present in the film due to the addition of Mn acts to stablize the internal polarization, accounting for the increase in the pyroelectric coefficient. The pyroelectric coefficient can be further improved by increasing the film annealing temperature from 530 to 560°C [33]. At 560°C, the dielectric constant and loss of the film are virtually the same as those at 530°C but the pyroelectric coefficient increased to 3.52 $\times$ 10^{-4} CK^{-1} m^{-2}. The FoM of this film is increased to 3.85×10^{-5} $Pa^{-0.5}$, one of the largest values reported for a thin film material, and comparable with some of the best bulk ceramics.

5. Conclusions

The criteria for the selection of ferroelectric materials for use in thermal detector arrays for such applications as thermal imaging and people counting have been reviewed. It has been shown that excellent properties can be obtained through the use of perovskite ceramics and thin films, especially modified lead zirconate and lead titanate based compositions. The importance of measuring the dielectric properties at an appropriate frequency (usually a few 10's Hz) has been emphasised. It has been indicated how material characteristics other than just the pyroelectric and dielectric properties are important in determining the performance of a device. The electrical resistivity can be especially important and it has been shown that specific off-valent donor dopants can be useful in determining the ceramic resistivities in a very well-controlled way. PMZT thin films can be made at relatively low temperatures (560°C) with pyroelectric properties that approach those of bulk ceramics.

Acknowledgments

The financial support of EPSRC for parts of this work through grants GR/ GR/R43303/01 and GR/N06113 is gratefully acknowledged.

References

1. S.B. Lang, *Ferroelectrics*, **230**, 401 (1999).
2. Y. Ta, *Comptes Rendus de l'Academie des Sciences*, **207**, 1042 (1938).
3. J. Cooper, *Rev. Sci. Instrum*., **33**, 92 (1962).
4. E.H. Putley, in *Semiconductors and Semimetals*, edited by R.K. Willardson and A.C. Beer (Academic Press, New York, 1970), vol. 5 p. 259
5. A. Hadni, R. Thomas, J. Mangin, and M. Bagard, *Infra-Red Phys*., **18**, 663 (1978).
6. M.R. Webb, *International J. Infrared and Millimeter Waves*, **12**, 1225 (1991).
7. C.B. Roundy, R.L. Byer, D.W. Phillion, and D. Kuizenga, *Opt. Commun*., **10**, 374 (1974).
8. R.W. Whatmore and R. Watton, in *Infrared Detectors and Emitters: Materials and Devices*, edited by P. Capper and C.T. Elliott (Chapman and Hall, London, 2000), p. 99.
9. M.V. Bennett and I. Matthews, *Proc. SPIE*., **2744**, 549 (1996).
10. C.M. Hanson, H.R. Beretan, J.F. Belcher, K.R. Udayakumar, and K.L. Soch, *Proc. SPIE*, **3379**, 60 (1998).
11. M.V. Mansi, S.G. Porter, J.L Gallowy, and N. Sumpter, in *Proc. SPIE Infra-red Technology and Applications*, XXVII April (2001).
12. R. Watton, P.A. Manning, M.C.J. Perkins, J.P. Gillham, and M.A. Todd, *Proc. SPIE XXII Infrared Technology and Applications*, **2744**, 486 (1996).
13. S.G. Porter, *Ferroelectrics*, **33**, 193 (1981).
14. R.W. Whatmore, *Reports on Progress in Physics*, **49**, 1335 (1986).
15. N.M Shorrocks., R.W. Whatmore, M.K. Robinson, and S.G. Porter, *Proc. SPIE*, **588**, 44 (1985).
16. R.W. Whatmore and F.W. Ainger, *Proc. SPIE*, **395**, 261 (1983).
17. R.W. Whatmore and A.J. Bell, *Ferroelectrics*, **35**, 155 (1983).
18. M. Nakamoto, N. Ichinose, N. Iwase, and Y. Yamashita, *J. Ceram. Soc. Jpn*., **110**, 639 (2002).
19. N.M. Shorrocks, R.W. Whatmore, and P.C. Osbond, *Ferroelectrics*, **106**, 387 (1990).
20. B.M. Kulwicki, A. Amin, H.R. Beratan, and C.M. Hanson, in *Proc. 8th International Symposium on Applications of*

Ferroelectrics (Greenville, SC, USA, Aug. 30 to Sept. 2 1992 IEEE Cat. No.90CH3080-9) (1992), p.1.
21. R. Clarke, A.M. Glazer, F.W. Ainger, D. Appleby, N.J. Poole, and S.G. Porter, *Ferroelectrics*, **11**, 359 (1976).
22. C.P. Shaw, S. Gupta, S.B. Stringfellow, A. Navarro, J.R. Alcock, and R.W. Whatmore , *J. European Ceram. Soc*., **22**, 2123 (2002).
23. F. Kulscar, US Patent 3,006,857 (1961).
24. A.J. Bell and R.W.Whatmore, *Ferroelectrics*, **37**, 543 (1981).
25. R.W.Whatmore and A.J. Bell, *Ferroelectrics*, **35**, 155 (1981).
26. R.W. Whatmore, *Ferroelectrics*, **49**, 201 (1983).
27. S.B. Stringfellow, S. Gupta, C. Shaw, J.R. Alcock, and R.W. Whatmore, *J. European Ceram. Soc*., **22**, 573 (2002).
28. R.W. Whatmore, O. Molter, and C.P. Shaw, *J. European Ceram. Soc*., **23**, 721 (2003).
29. Y.J. Wu, N. Uekawa, K. Kakegawa, and Y. Sasaki, *Key Engineering Materials*, **228/229**, 3 (2002).
30. H. Komiya, Y. Naito, T. Takenaka, and K. Sakata, *Jpn. J. Appl. Phys*., **28**, 114 (1989).
31. A. Navarro, J.R. Alcock, and R.W. Whatmore, in *Proc. ICE 2003* (2003).
32. Q. Zhang and R.W. Whatmore, *J. Phys. D: Appl. Phys*., **34**, 2296 (2001).
33. Q. Zhang and R.W. Whatmore, *J. Appl. Phys*. Accepted for publication (2003).